Ultrasound Obstet Gynecol 2023; **61**: 765–772
Published online in Wiley Online Library (wileyonlinelibrary.com). **DOI:** 10.1002/uog.26192.

Phase-rectified signal averaging: correlation between two monitors and relationship with short-term variation of fetal heart rate

B. LIU[1,2], B. THILAGANATHAN[1,2] and A. BHIDE[1,2]

[1]*Fetal Medicine Unit, St George's University Hospitals NHS Foundation Trust, London, UK;* [2]*Vascular Biology Research Centre, Molecular and Clinical Sciences Research Institute, St George's University of London, London, UK*

KEYWORDS: ambulatory monitoring; computerized cardiotocography; fetal heart-rate monitoring; non-invasive fetal electrocardiography; phase-rectified signal averaging; short-term variation

CONTRIBUTION

What are the novel findings of this work?
Phase-rectified signal averaging (PRSA) indices obtained using non-invasive fetal electrocardiography (NIFECG) and computerized cardiotocography are highly correlated. PRSA also has a strong linear relationship with short-term variation (STV), demonstrating its potential to assess fetal autonomic wellbeing.

What are the clinical implications of this work?
Due to its in-built ability to eliminate noise, PRSA can account for the dynamic nature of NIFECG and generate outputs of higher accuracy and number compared with STV. PRSA may permit self-applied remote fetal monitoring using NIFECG, thus facilitating increased fetal surveillance in high-risk women without increasing service demands.

ABSTRACT

Objectives *To establish the correlation between phase-rectified signal averaging (PRSA) outputs obtained from a novel self-applicable non-invasive fetal electrocardiography (NIFECG) monitor with those from computerized cardiotocography (cCTG). A secondary objective was to evaluate the potential for remote assessment of fetal wellbeing by determining the relationship between PRSA and short-term variation (STV).*

Methods *This was a prospective observational study of women with a singleton pregnancy over 28 + 0 weeks' gestation attending a London teaching hospital for cCTG assessment. Participants underwent concurrent cCTG and NIFECG monitoring for up to 60 min. Averaged accelerative (AAC) and decelerative (ADC) capacities and STV were derived by postprocessing and filtration of signals, generating fully (F) and partially (P) filtered results. Linear correlation and accuracy and precision analysis were performed to assess the relationship between PRSA outputs from cCTG and NIFECG, using varying anchor thresholds, and their association with STV.*

Results *A total of 306 concurrent cCTG and NIFECG traces were collected from 285 women. F-filtered NIFECG PRSA (eAAC/eADC) results were generated from 65% of traces, whereas cCTG PRSA (cAAC/cADC) outputs were generated from all. Strong correlations were observed between cAAC and F-filtered eAAC ($r = 0.879$, $P < 0.001$) and between cADC and F-filtered eADC ($r = 0.895$, $P < 0.001$). NIFECG anchor detection decreased significantly with increasing signal loss, and NIFECG PRSA indices showed considerable deviation from those of cCTG when derived from traces in which fewer than 100 anchors were detected. Removing anchor filters from NIFECG traces to generate P-filtered PRSA outputs weakened the correlation (AAC: $r = 0.505$, $P < 0.001$; ADC: $r = 0.560$, $P < 0.001$). Lowering the anchor threshold to 100 increased the yield of eAAC and eADC outputs to approximately 74%, whilst maintaining strong correlation with cAAC ($r = 0.839$, $P < 0.001$) and cADC ($r = 0.815$, $P < 0.001$), respectively. Both cAAC and cADC showed a very strong linear relationship with cCTG STV ($r = 0.928$, $P < 0.001$ and $r = 0.911$, $P < 0.001$, respectively). Similar findings were observed with eAAC ($r = 0.825$, $P < 0.001$) and eADC ($r = 0.827$, $P < 0.001$).*

Correspondence to: Dr A. Bhide, Fetal Medicine Unit, Department of Obstetrics and Gynaecology, St George's University Hospitals NHS Foundation Trust, Blackshaw Road, London SW17 0QT, UK (e-mail: abhide@sgul.ac.uk)

Accepted: 14 February 2023

Conclusions *PRSA appears to be a method of fetal assessment equivalent to STV, but, due to its innate ability to eliminate artifacts, it generates interpretable NIFECG traces with high accuracy at a higher rate. These findings raise the possibility of self-applied at-home or remote fetal heart-rate monitoring with automated reporting, thus enabling increased surveillance in high-risk women without impacting on service demand.* © *2023 The Authors. Ultrasound in Obstetrics & Gynecology published by John Wiley & Sons Ltd on behalf of International Society of Ultrasound in Obstetrics and Gynecology.*

INTRODUCTION

Placental dysfunction remains a major health concern in pregnancy, manifesting in fetal growth restriction (FGR), chronic fetal hypoxemia and stillbirth[1,2]. Chronic hypoxemia can be assessed using methods including fetal Doppler assessment and fetal heart-rate (FHR) analysis on cardiotocography (CTG). As fetal hypoxemia worsens, FHR variability declines[3,4]. Computerized CTG (cCTG) generates numerical outputs for FHR parameters, allowing standardized interpretation and minimizing inaccuracies associated with visual CTG analysis[5,6]. A key output is short-term variation (STV), which evaluates fetal autonomic activity by averaging the differences in mean pulse interval between 3.75-s epochs over 1 min and then over an entire trace[7]. STV has been shown to be a vital and reliable indicator of fetal hypoxia[6–9].

More recently, phase-rectified signal averaging (PRSA) has emerged as a new method for fetal autonomic assessment. PRSA evaluates the speed of FHR change within quasiperiodic oscillations in a time series, producing numerical values that characterize accelerations (averaged accelerative capacity (AAC)) and decelerations (averaged decelerative capacity (ADC)). These indices allow the sympathetic and parasympathetic influences on cardiac modulation to be studied as separate entities, whilst also accounting for non-stationary signals and eliminating noise[10–14]. Application of PRSA to adult electrocardiography (ECG) recordings demonstrated the value of decelerative capacity in predicting mortality following myocardial infarction[15]. The utility of PRSA in autonomic assessment has prompted its evaluation in FHR monitoring, with evidence suggesting that it may be superior to STV in detecting evolving fetal hypoxia[12–14,16].

Current fetal wellbeing assessments are hospital-based and limited by the availability of appointments and skilled personnel. The development of a reliable method of remote FHR monitoring with accurate automated outputs would enable increased fetal surveillance in high-risk pregnancies. Non-invasive fetal ECG (NIFECG) can be self-applied as it does not require placement in proximity to the fetal heart; it also minimizes fetal–maternal heart-rate confusion and is not affected by maternal adiposity[17–20]. It is conceivable that a key challenge associated with deriving STV, namely susceptibility to artifacts, may be overcome by the innate ability of PRSA to eliminate noise[21,22]. The objective of this study was to compare PRSA values obtained by cCTG with those from a novel self-applied NIFECG device. A secondary objective was to evaluate the relationship between PRSA and STV values.

METHODS

This was a single-center prospective cohort study of patients attending St George's University Hospitals NHS Foundation Trust, London, UK, between June 2021 and June 2022. Women with a singleton pregnancy over 28 + 0 weeks' gestation who presented requiring cCTG monitoring for any clinical indication were eligible, providing written informed consent was obtained. Concurrent monitoring using both cCTG (Sonicaid FM800 Encore Fetal Monitor; Huntleigh Healthcare Ltd., Cardiff, UK) and a novel self-applicable NIFECG device (Femom™; Biorithm Pte Ltd., Singapore) was performed for up to 60 min. The NIFECG device is designed to produce automated FHR outputs in the remote setting, with self-application by the patient and remote clinician assessment, and is particularly relevant for high-risk women. NIFECG data were extracted in BioCapture recording files (.bcrx) and, following signal processing, exported as comma separated value (.csv) files, producing FHR values for each 0.25-s epoch. Similar .csv files were also exported from each concurrent cCTG trace. Full inclusion criteria, device information and data acquisition methods are detailed in our study protocol[23]. Ethical approval was obtained from South East Scotland Research Ethics Committee 2 (REC reference 19/SS/0109, IRAS ID 260032) and MHRA (CI/2020/0028).

Signal processing

NIFECG traces were sampled at a frequency of 500 Hz. FHR data generated by a sequence of maternal R-wave removal, fetal R-wave signal enhancement and R–R interval calculation were in turn sampled at 4 Hz, with one FHR value expressed per 0.25-s epoch. cCTG sampling at 4 Hz produced smoothed FHR values, which were also displayed in 0.25-s epochs. Signal acquisition in NIFECG was defined as FHR within a valid range. Signal loss was defined as FHR outliers < 30 bpm or > 240 bpm. All FHR values were converted to fetal R–R intervals (FRR) and expressed in ms.

STV computation

For cCTG, STV (cSTV) was computed as described by Dawes *et al.*[5], in which differences in mean pulse interval between successive 3.75-s epochs were averaged for each trace[6,7]. NIFECG STV (eSTV) was derived using a similar processing method. For optimal accuracy, three filters were applied at three different stages of the processing algorithm to remove traces or trace

sections containing > 50% signal loss, producing fully (F) filtered eSTV values. Partially (P) filtered eSTV values were generated without the application of these filters, instead using only an outlier filter. Our research showed weak correlation between P-filtered eSTV and cSTV ($R = 0.337$, $P < 0.001$), but strong correlation when using F-filtered eSTV ($R = 0.911$, $P < 0.001$)[24]. For this reason, only F-filtered eSTV was compared against PRSA values from the two monitors.

PRSA computation

PRSA processing followed the steps and definitions reported by Huhn *et al.*[13], and was performed for both NIFECG and cCTG recordings (outputs were termed eAAC/eADC and cAAC/cADC, respectively). The parameter T refers to the number of FRR intervals that are averaged to produce each T-value, which are used to identify anchors (points of acceleration/deceleration). Using $T = 40$ in our algorithm meant that FRR was averaged over 40 samples i.e. a 10-s window (4 Hz = 4 samples/s). The parameter L is the length of the time window around an anchor point, expressed in s. We used $L = 200$ in our algorithm, meaning that a 200-s window was extracted around each anchor (100 s before and 100 s after the anchor). The parameter S is size of the segment around the final aligned anchor, in terms of the number of samples on either side, which was required to compute AAC/ADC. In our equation, $S = 40$.

AAC values for each trace were generated using the following steps: (1) FRR was averaged over 40 sampling points (10-s windows) to derive T-values, and windows containing > 20% artifacts/outliers, defined as FRR < 250 ms or > 2000 ms (i.e. FHR > 240 bpm or < 30 bpm), were excluded; (2) a decrease between any two consecutive T-values was assigned an anchor between the two values; (3) a 200-s time window was selected around each anchor, with the potential for overlap between windows of adjacent anchors; (4) all 200-s windows were aligned by anchor points; (5) a PRSA waveform was obtained by averaging all aligned waveforms; and (6) AAC was quantified as the difference between the mean of the 39 ($S - 1$) samples before and that of the 39 samples after the aligned anchor. ADC was calculated in the same fashion, but anchors were defined between consecutive increasing T-values in step 2 above[11–13].

AAC outputs were negative as they captured reductions in FRR, but absolute AAC values are reported in this paper for simplicity. Huhn *et al.*[13] removed T-values (averaged 10-s windows) with a difference of > 5% from the preceding T-value for CTG PRSA computation, while we adopted a different approach of removing 10-s windows containing > 20% outliers (FRR < 250 ms or > 2000 ms). Two filters were applied during the processing of AAC and ADC to remove spurious and inaccurate results caused by artifacts and signal loss. If the entire trace had > 80% signal loss and/or if fewer than 400 anchors were detectable, eAAC and eADC values were not generated. Thus, only traces with low levels of signal loss generated a F-filtered PRSA output. The number of anchors detected for each NIFECG trace was recorded. P-filtered eAAC and eADC values were generated without the anchor filter (i.e. using traces with any number of detectable anchors). Various anchor thresholds were applied to the P-filtered dataset to define the best filter for maximizing data output whilst maintaining correlation with cAAC/cADC. As cCTG has a lower level of signal loss due to autocorrelation, we anticipated high numbers of anchors being detected in each trace, therefore the analysis of anchor count was not performed for cCTG traces.

Statistical analysis

Descriptive data are presented as median (interquartile range (IQR)) for continuous variables and n (%) for categorical variables. Linearity of AAC/ADC and STV values derived from the two devices by various methods of computation was established using Pearson's correlation coefficient, after confirming normality using the Kolmogorov–Smirnov test. Accuracy and precision analysis was carried out to assess the mean bias, precision (expressed as SD) and 95% upper and lower limits of agreement (LoA) for each method of eAAC/eADC computation and cAAC/cADC. The statistical software package SPSS version 28.0 (SPSS Corp., Armonk, NY, USA) was used for the analysis. P-values < 0.05 were considered significant.

RESULTS

Concurrent NIFECG and cCTG monitoring was undertaken in 285 women, with a total of 306 traces collected from each machine. This study population was also used to investigate characteristics associated with NIFECG signal loss[25] and correlation between STV computed by NIFECG and cCTG[24]. Maternal and pregnancy characteristics are outlined in Table S1.

PRSA signal processing

Final AAC and ADC waveforms generated by signal averaging are displayed in Figure 1. As NIFECG is prone to artifacts and outliers, many traces did not fulfil the filtering requirements. Applying the PRSA anchor filter to 306 NIFECG traces produced eAAC values in 200 (65.4%) traces and eADC values in 201 (65.7%) (Table 1). Median eAAC and eADC were 5.5 (IQR, 4.5–6.7) ms and 5.9 (IQR, 4.6–7.4) ms, respectively. Removal of filters increased the number of outputs generated (eAAC, 255/306 (83.3%); eADC, 256/306 (83.7%)). There were fewer FHR outliers in cCTG data, so outputs were generated from all traces. Median values of cAAC and cADC were 5.8 (IQR, 4.6–7.0) ms and 6.1 (IQR, 4.8–7.7) ms, respectively. STV values were obtained from 46.4% of F-filtered and 98.4% of P-filtered NIFECG traces and 100% of cCTG traces. Median STV values from the two monitors are displayed in Table 1.

PRSA agreement and anchor threshold definition

The agreement between AAC/ADC values obtained from the two monitors, using F- and P-filtered processing algorithms, is shown in Table 2. F-filtered eAAC and eADC were correlated strongly with cAAC ($r = 0.879$, $P < 0.001$) and cADC ($r = 0.895$, $P < 0.001$), respectively. Mean bias and LoA for F-filtered eAAC and cAAC are shown in the Bland–Altman plot in Figure 2. Correlation with cCTG was weaker for P-filtered eAAC ($r = 0.505$, $P < 0.001$) and eADC ($r = 0.560$, $P < 0.001$). Accuracy and precision analysis also indicated poorer agreement once the anchor filters were removed.

Using the method outlined by Huhn *et al.*[13] of removing 10-s windows with > 5% change from the previous *T*-value, AAC and ADC from the two monitors were poorly correlated (cAAC *vs* eAAC: $r = 0.206$, $P < 0.001$; cADC *vs* eADC: $r = 0.203$, $P < 0.001$). Relaxing our outlier threshold for window removal from > 20% to > 30% also weakened correlation for AAC ($r = 0.206$, $P < 0.001$) and ADC ($r = 0.413$, $P < 0.001$). Tightening the outlier threshold to > 10% generated fewer PRSA outputs (78.8% *vs* 83.7%).

Figure 3 illustrates all anchors detected in a high-quality NIFECG trace section. The number of AAC anchors detected against the percentage of signal loss in each

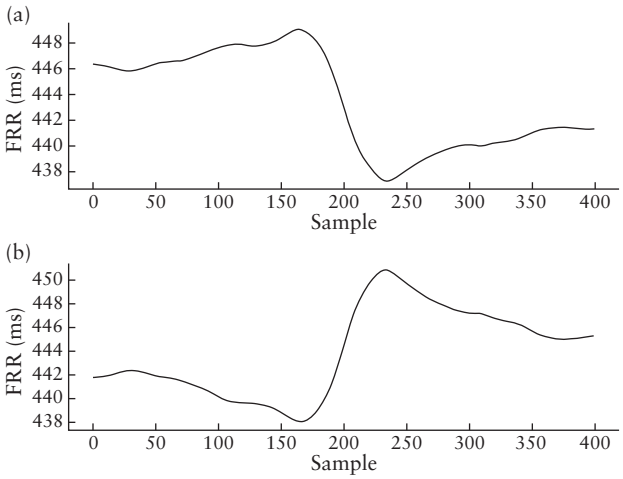

Figure 1 Final averaged accelerative capacity (a) and averaged decelerative capacity (b) waveforms generated by phase-rectified signal averaging of traces sampled at 4 Hz (4 samples/s). FRR, fetal R–R interval.

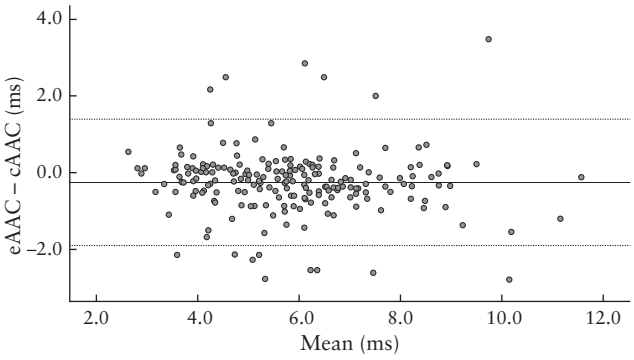

Figure 2 Bland–Altman plot showing mean bias (——) and 95% limits of agreement (·····) in averaged accelerative capacity derived from computerized cardiotocography (cAAC) and non-invasive fetal electrocardiography (eAAC).

Table 1 Characteristics of phase-rectified signal averaging (PRSA) and short-term variation (STV) outputs generated from 306 concurrent computerized cardiotocography (cCTG) and non-invasive fetal electrocardiography (NIFECG) traces, using fully (F) and partially (P) filtered processing algorithms

Output	*cCTG*	*NIFECG F-filtered*	*NIFECG P-filtered*
PRSA			
Traces producing AAC	306 (100.0)	200 (65.4)	255 (83.3)
Traces producing ADC	306 (100.0)	201 (65.7)	256 (83.7)
AAC (ms)	5.8 (4.6–7.0)	5.5 (4.5–6.7)	5.6 (4.5–7.0)
ADC (ms)	6.1 (4.8–7.7)	5.9 (4.6–7.4)	5.9 (4.6–7.7)
STV			
Traces	306 (100.0)	142 (46.4)	301 (98.4)
STV (ms)	9.9 (7.9–12.3)	9.2 (7.6–11.4)	10.7 (8.6–13.7)

Data are given as *n* (%) or median (interquartile range). AAC, averaged accelerative capacity; ADC, averaged decelerative capacity.

Table 2 Linear correlation, accuracy and precision analysis for fully (F) and partially (P) filtered phase-rectified signal averaging outputs obtained on non-invasive fetal echocardiography (NIFECG) compared with computerized cardiotocography (cCTG)

Output	n	*Pearson's* r *coefficient**	*Mean bias (ms)*	*95% LoA (ms)*	*Precision (ms)*
cAAC *vs* F-filtered eAAC	200	0.879	−0.255	−1.917 to 1.407	0.848
cADC *vs* F-filtered eADC	201	0.895	−0.283	−2.094 to 1.528	0.924
cAAC *vs* P-filtered eAAC	255	0.505	0.191	−4.685 to 5.067	2.488
cADC *vs* P-filtered eADC	256	0.560	0.062	−5.293 to 5.417	2.732

cAAC, averaged accelerative capacity on cCTG; cADC, averaged decelerative capacity on cCTG; eAAC, averaged accelerative capacity on NIFECG; eADC, averaged decelerative capacity on NIFECG; LoA, limits of agreement. *All *P*-values < 0.001.

NIFECG trace is shown in Figure 4 (a similar pattern was observed for ADC anchors). In traces with close to 80% signal loss, very few anchors were detectable. The difference between monitors in AAC (eAAC – cAAC) (Figure 5) and ADC (eADC – cADC) increased significantly when fewer than 100 anchors were detected.

In order to increase eAAC and eADC outputs whilst maintaining strong correlation with cAAC and cADC, respectively, exclusion thresholds were applied at 100, 200, 300 and 400 (original filter) detected anchors. Agreement in AAC and ADC values between monitors was evaluated for NIFECG traces containing more than

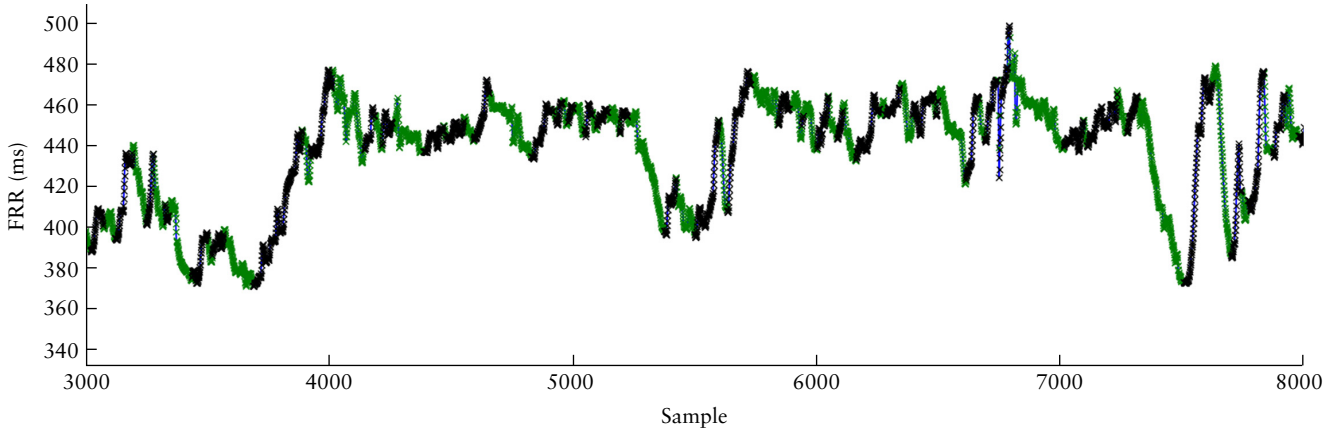

Figure 3 Averaged accelerative capacity (×) and averaged decelerative capacity (×) anchors derived from a non-invasive fetal electrocardiography trace section sampled at 4 Hz (4 samples/s). FRR, fetal R–R interval.

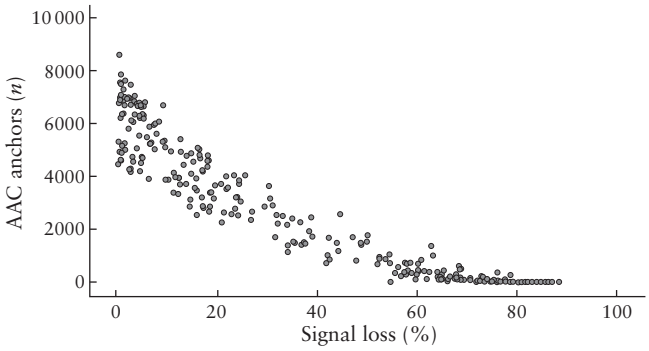

Figure 4 Scatterplot demonstrating relationship between number of averaged accelerative capacity (AAC) anchors detected and percentage signal loss for traces obtained by non-invasive fetal electrocardiography. Traces with > 80% signal loss were automatically assigned zero anchors.

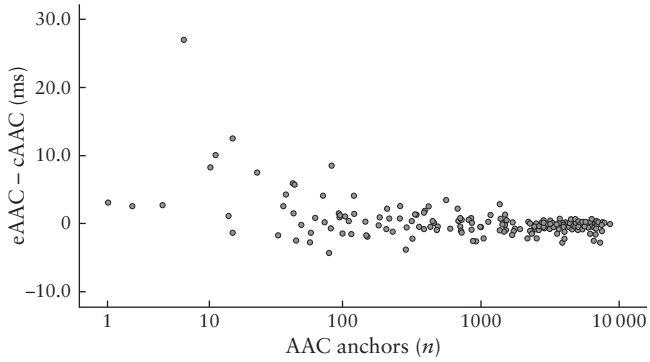

Figure 5 Scatterplot demonstrating relationship between difference in averaged accelerative capacity (AAC) obtained by computerized cardiotocography (cAAC) *vs* non-invasive fetal electrocardiography (eAAC) and number of anchors detected. Logarithmic scale is used due to large range in number of anchors.

Table 3 Linear correlation, accuracy and precision analysis for partially filtered phase-rectified signal averaging (PRSA) outputs obtained on non-invasive fetal echocardiography (NIFECG), using various anchor thresholds, against PRSA outputs obtained on computerized cardiotocography (cCTG)

Threshold	*Traces* (n *(%)*)	*Pearson's* r *coefficient**	*Mean bias (ms)*	*95% LoA (ms)*	*Precision (ms)*
eAAC *vs* cAAC					
> 400 anchors	200 (65.4)	0.879	−0.255	−1.917 to 1.407	0.848
> 300 anchors	207 (67.6)	0.877	−0.240	−1.947 to 1.467	0.871
> 200 anchors	215 (70.3)	0.858	−0.231	−2.060 to 1.598	0.933
> 100 anchors	225 (73.5)	0.839	−0.208	−2.141 to 1.725	0.986
eADC *vs* cADC					
> 400 anchors	201 (65.7)	0.895	−0.283	−2.094 to 1.528	0.924
> 300 anchors	207 (67.6)	0.874	−0.235	−2.228 to 1.758	1.017
> 200 anchors	216 (70.6)	0.857	−0.200	−2.356 to 1.956	1.100
> 100 anchors	229 (74.8)	0.815	−0.084	−2.616 to 2.448	1.292

cAAC, averaged accelerative capacity on cCTG; cADC, averaged decelerative capacity on cCTG; eAAC, averaged accelerative capacity on NIFECG; eADC, averaged decelerative capacity on NIFECG; LoA, limits of agreement. *All *P*-values < 0.001.

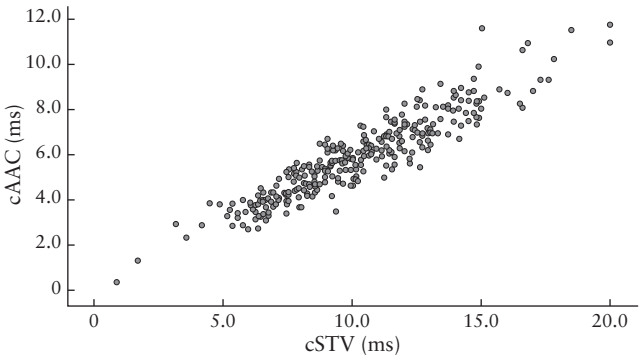

Figure 6 Scatterplot showing correlation between averaged accelerative capacity (cAAC) and short-term variation (cSTV) obtained on computerized cardiotocography ($r = 0.928$).

Table 4 Linear correlation between short-term variation (STV) and phase-rectified signal averaging (PRSA) outputs obtained on computerized cardiotocography (cCTG) and fully filtered non-invasive fetal electrocardiography (NIFECG)

	STV	
PRSA	*cCTG*	*NIFECG*
cAAC	0.928	0.838
cADC	0.911	0.834
eAAC	0.825	0.874
eADC	0.827	0.849

cAAC, averaged accelerative capacity on cCTG; cADC, averaged decelerative capacity on cCTG; eAAC, averaged accelerative capacity on NIFECG; eADC, averaged decelerative capacity on NIFECG. All *P*-values < 0.001.

the aforementioned numbers of anchors (Table 3). Linear correlation between eAAC and cAAC and between eADC and cADC remained strong with reduced anchor thresholds. Compared with the original filter, using a threshold of > 100 anchors yielded eAAC and eADC results from a higher number of traces (225/306 (73.5%) and 229/306 (74.8%), respectively), whilst correlation with cAAC and cADC showed little change ($r = 0.839$, $P < 0.001$ and $r = 0.815$, $P < 0.001$, respectively). Mean bias, precision and LoA did not change significantly when anchor thresholds were reduced.

Correlation of PRSA with STV

A very strong correlation was observed between cSTV and both cAAC ($n = 306$, $r = 0.928$, $P < 0.001$) and cADC ($n = 306$, $r = 0.911$, $P < 0.001$) (Figure 6 and Table 4). F-filtered eAAC and eADC were also correlated strongly with cSTV ($r = 0.825$, $P < 0.001$ and $r = 0.827$, $P < 0.001$, respectively). Similarly, both eAAC/eADC and cAAC/cADC were correlated strongly with F-filtered eSTV (Table 4).

DISCUSSION

NIFECG reliably produced PRSA values that correlated highly with both PRSA and STV values obtained using cCTG. Reducing the threshold during PRSA processing from > 400 detectable anchors to > 100 optimized PRSA yield whilst maintaining concordance with cCTG PRSA values. Interpretable PRSA outputs were generated more frequently from F-filtered NIFECG compared with STV. The strong correlation of PRSA with STV suggests that PRSA may accurately reflect fetal autonomic status.

PRSA signal processing

NIFECG samples FHR at a frequency of 500 Hz and is prone to artifacts, electrical interference and poor fetal R-wave detection[21,22]. In contrast, cCTG cannot sample at such high frequencies so uses autocorrelation to produce smoothed FHR at a frequency of 4 Hz. Thus, FHR values from each 0.25-s epoch in NIFECG traces will be naturally more fluctuant compared with those derived from cCTG. Higher values of the parameters *T* and *S* allow more FHR samples to be averaged in each window, reducing the likelihood of major fluctuations in NIFECG traces. This was demonstrated by another study that compared PRSA outputs from CTG and NIFECG, using different parameter settings[26]. On evaluating 28 concurrent FHR recordings, taken from nine growth-restricted and four appropriate-for-gestational-age (AGA) fetuses, strong correlation of AAC/ADC between the two monitors was observed only when *T* and *S* parameters were set at values greater than 40 ($r > 0.8$), whilst correlation was weak when *T* and *S* were less than five ($r < 0.1$)[26]. As the parameter *L* simply defines the window size for anchor alignment, it does not influence the output.

The method proposed by Huhn *et al.*[13] of removing *T*-values with > 5% change from the preceding *T*-value was developed originally for cCTG. Removing 10-s windows with > 20% outliers is in line with the method of outlier removal in ECG processing described by Bauer *et al.*[10]. Our correlation analysis demonstrated the superiority of this method, as it accounted for greater fluctuations in NIFECG, and that a 20% outlier threshold maximized PRSA output whilst maintaining strong correlation with cCTG. Various algorithms, outlier thresholds and values for *T* and *S* parameters have been tested and applied to cCTG and fetal ECG outputs[11,14,26], and several proposals have been put forward for the best parameter settings. Given the requirement for high *T* and *S* values in NIFECG signal processing, and the near-perfect correlation evident between cSTV and cAAC/cADC using parameter values set by Huhn *et al.*[13], $T = 40$ and $S = 40$ appear to be the most appropriate settings for the assessment of fetal hypoxemia.

Clinical implications

Previous comparisons have been made in FGR and AGA fetuses, of which all concluded that PRSA had superior diagnostic power compared with STV in detecting FGR and/or predicting neonatal morbidity[11–13,27]. Lobmaier *et al.*[16] demonstrated that, in longitudinal cCTG recordings from 279 severe early-onset FGR fetuses,

cAAC/cADC declined 72 h prior to elective birth, whereas the decline in STV became significant fewer than 48 h before birth. As our dataset captured a routine patient cohort, we did not include adequate numbers of pregnancies with FGR or adverse outcomes to perform a similar comparison. The largest retrospective study evaluating PRSA in FHR monitoring is that of Georgieva *et al.*[14], who applied the PRSA algorithm to 7568 intrapartum cCTG traces 30 min prior to delivery. Increased cADC predicted acidemia at birth significantly better than did STV (area under the receiver-operating-characteristics curve (AUC), 0.665 *vs* 0.606, $P < 0.001$). Unlike in this study, the authors observed a weak correlation between STV and cAAC/cADC ($r = 0.29$)[14]. This may be a result of the different values used in their computation for parameters T and L (5 and 45, respectively). It could also relate to the reduced accuracy of STV in the active second stage of labor, due to high signal loss and a high incidence of decelerations. The mechanism of intrapartum acidosis is more likely attributable to acute or subacute hypoxia as opposed to chronic hypoxia, thereby increasing FHR variability[28]. Indeed, other antepartum studies have demonstrated stronger correlations between STV and cAAC/cADC[12,13]. Another intrapartum study compared PRSA and STV outputs obtained from cCTG in 227 neonates born with acidemia against those obtained in 227 controls[29]. This study also found that ADC was significantly higher in those born with low umbilical artery pH and was a better predictor of fetal acidosis than was STV (AUC, 0.659 *vs* 0.566, $P = 0.013$).

Due to the strong linear relationship with STV demonstrated in the present cohort, it would be reasonable to conclude that PRSA, with the appropriate computation, is equivalent to STV in assessing fetal autonomic status. Given the algorithm's innate ability to remove noise and artifacts, PRSA can provide higher accuracy and more outputs from NIFECG compared with STV. Although some authors have proposed a PRSA reference range, these were based on small sample sizes and have not been validated[12,27]. Until a validated reference standard exists, the linear relationship with STV may enable PRSA thresholds to be set according to the correlating STV value. Similarly, due to the difficulties encountered in our analysis in accurate STV computation from NIFECG, STV values could be derived from eAAC/eADC outputs.

Strengths and limitations

This study evaluated systematically PRSA outputs from two monitors and used appropriate thresholds and algorithms that accounted specifically for the dynamic nature of NIFECG. We further improved PRSA output generation by pinpointing the exact cause for any inaccuracy. The application of PRSA to cCTG resulted in high correlation with STV, which is the current gold standard for detecting hypoxia based on FHR. Comparison with pregnancies complicated by placental insufficiency or those with adverse outcome may have offered more insight into the diagnostic accuracy of PRSA, but due to our patient sample, this could not be performed. Further research with a large, healthy cohort is required to establish and validate a reference standard.

Conclusions

PRSA appears to be a method of assessing fetal wellbeing equivalent to STV. With appropriate computation and signal processing to account for the difference in technology, NIFECG PRSA outputs are correlated strongly with cCTG PRSA and STV. Due to its in-built ability to eliminate artifacts, PRSA analysis from the dynamic NIFECG may eventually replace STV in FHR monitoring, as the latter has demonstrated low accuracy and few outputs in poor-quality traces. These findings raise the potential for accurate, automated at-home FHR assessment using self-applied NIFECG, thereby improving fetal surveillance in high-risk women without increasing service demands.

ACKNOWLEDGMENTS

We acknowledge our commercial sponsors, Biorithm Pte Ltd, for funding this study, and the Bioengineering team for analyzing the traces acquired and refining the processing algorithms. We also thank the following midwives for identifying eligible women and helping with recruitment: Melissa Ogbomo, Maria Gutierrez-Vuong, Deborah Brown, Simone Schloss, Zainab Anidugbe, Yasmin Yussuff-Jakkari, Marta Hernandez, Ines Moya Sanchez, Inma Clavijo and Manette Lindsay. The sponsors had no role in the study design, recruitment, data acquisition or write-up.

REFERENCES

1. Liu B, Nadeem U, Frick A, Alakaloko M, Bhide A, Thilaganathan B. Reducing health inequality in Black, Asian and other minority ethnic pregnant women: impact of first trimester combined screening for placental dysfunction on perinatal mortality. *BJOG* 2022; **129**: 1750–1756.
2. Poon LC, Shennan A, Hyett JA, Kapur A, Hadar E, Divakar H, McAuliffe F, da Silva Costa F, von Dadelszen P, McIntyre HD, Kihara AB, Di Renzo GC, Romero R, D'Alton M, Berghella V, Nicolaides KH, Hod M. The International Federation of Gynecology and Obstetrics (FIGO) initiative on pre-eclampsia: A pragmatic guide for first-trimester screening and prevention. *Int J Gynaecol Obstet* 2019; **145**: 1–33.
3. Ayres-de-Campos D, Spong CY, Chandraharan E. FIGO consensus guidelines on intrapartum fetal monitoring: Cardiotocography. *Int J Gynecol Obstet* 2015; **131**: 13–24.
4. Chandraharan E. *Handbook of CTG Interpretation: From Patterns to Physiology*. Cambridge University Press: Cambridge, 2017. DOI: 10.1017/9781316161715.
5. Dawes GS, Lobb M, Moulden M, Redman CWG, Wheeler T. Antenatal cardiotocogram quality and interpretation using computers. *BJOG* 2014; **121**: 2–8.
6. Pardey J, Moulden M, Redman CWG. A computer system for the numerical analysis of nonstress tests. *Am J Obstet Gynecol* 2002; **186**: 1095–1103.
7. Street P, Dawes GS, Moulden M, Redman CWG. Short-term variation in abnormal antenatal fetal heart rate records. *Am J Obstet Gynecol* 1991; **165**: 515–523.
8. Bilardo CM, Wolf H, Stigter RH, Ville Y, Baez E, Visser GH, Hecher K. Relationship between monitoring parameters and perinatal outcome in severe, early intrauterine growth restriction. *Ultrasound Obstet Gynecol* 2004; **23**: 119–125.
9. Ribbert LS, Snijders RJ, Nicolaides KH, Visser GH. Relation of fetal blood gases and data from computer-assisted analysis of fetal heart rate patterns in small for gestation fetuses. *Br J Obstet Gynaecol* 1991; **98**: 820–823.
10. Bauer A, Kantelhardt JW, Bunde A, Barthel P, Schneider R, Malik M, Schmidt G. Phase-rectified signal averaging detects quasi-periodicities in non-stationary data. *Phys A Stat Mech Appl* 2006; **364**: 423–434.
11. Stampalija T, Casati D, Montico M, Sassi R, Rivolta MW, Maggi V, Bauer A, Ferrazzi E. Parameters influence on acceleration and deceleration capacity based on trans-abdominal ECG in early fetal growth restriction at different gestational age epochs. *Eur J Obstet Gynecol Reprod Biol* 2015; **188**: 104–112.
12. Lobmaier SM, Huhn EA, Pildner von Steinburg S, Müller A, Schuster T, Ortiz JU, Schmidt G, Schneider KT. Phase-rectified signal averaging as a new method for surveillance of growth restricted fetuses. *J Matern Neonatal Med* 2012; **25**: 2523–2528.

13. Huhn EA, Lobmaier S, Fischer T, Schneider R, Bauer A, Schneider KT, Schmidt G. New computerized fetal heart rate analysis for surveillance of intrauterine growth restriction. *Prenat Diagn* 2011; **31**: 509–514.
14. Georgieva A, Papageorghiou A, Payne S, Moulden M, Redman C. Phase-rectified signal averaging for intrapartum electronic fetal heart rate monitoring is related to acidaemia at birth. *BJOG* 2014; **121**: 889–894.
15. Bauer A, Kantelhardt JW, Barthel P, Schneider R, Mäkikallio T, Ulm K, Hnatkova K, Schömig A, Huikuri H, Bunde A, Malik M, Schmidt G. Deceleration capacity of heart rate as a predictor of mortality after myocardial infarction: cohort study. *Lancet* 2006; **367**: 1674–1681.
16. Lobmaier SM, Mensing van Charante N, Ferrazzi E, Giussani DA, Shaw CJ, Müller A, Ortiz JU, Ostermayer E, Haller B, Prefumo F, Frusca T, Hecher K, Arabin B, Thilaganathan B, Papageorghiou AT, Bhide A, Martinelli P, Duvekot JJ, van Eyck J, Visser GH, Schmidt G, Ganzevoort W, Lees CC, Schneider KT; TRUFFLE investigators. Phase-rectified signal averaging method to predict perinatal outcome in infants with very preterm fetal growth restriction: a secondary analysis of TRUFFLE-trial. *Am J Obstet Gynecol* 2016; **215**: 630.e1–7.
17. Reinhard J, Hayes-Gill BR, Schiermeier S, Hatzmann H, Heinrich TM, Louwen F. Intrapartum heart rate ambiguity: A comparison of cardiotocogram and abdominal fetal electrocardiogram with maternal electrocardiogram. *Gynecol Obstet Invest* 2013; **75**: 101–108.
18. Graatsma EM, Miller J, Mulder EJH, Harman C, Baschat AA, Visser GHA. Maternal body mass index does not affect performance of fetal electrocardiography. *Am J Perinatol* 2010; **27**: 573–577.
19. Huhn EA, Müller MI, Meyer AH, Manegold-Brauer G, Holzgreve W, Hoesli I, Wilhelm FH. Quality Predictors of Abdominal Fetal Electrocardiography Recording in Antenatal Ambulatory and Bedside Settings. *Fetal Diagn Ther* 2017; **41**: 283–292.
20. Graatsma EM, Jacod BC, Van Egmond LAJ, Mulder EJH, Visser GHA. Fetal electrocardiography: Feasibility of long-term fetal heart rate recordings. *BJOG* 2009; **116**: 334–337.
21. Sameni. A Review of Fetal ECG Signal Processing Issues and Promising Directions. *Open Pacing Electrophysiol Ther J* 2010; **3**: 4–20.
22. Clifford GD, Silva I, Behar J, Moody GB. Non-invasive fetal ECG analysis. *Physiol Meas* 2014; **35**: 1521–1536.
23. Liu B, Marler E, Thilaganathan B, Bhide A. Ambulatory antenatal fetal electrocardiography in high-risk pregnancies (AMBER): protocol for a pilot prospective cohort study. *BMJ Open* 2023; **13**: e062448.
24. Liu B, Thilaganathan B, Bhide A. Correlation of short-term variation derived from novel ambulatory fetal electrocardiography monitor with computerized cardiotocography. *Ultrasound Obstet Gynecol* 2023; **61**: 758–764.
25. Liu B, Thilaganathan B, Bhide A. Effectiveness of ambulatory non-invasive fetal electrocardiography: impact of maternal and fetal characteristics. *Acta Obstet Gynecol Scand* 2023; **102**: 577.
26. Van Scheepen JAM, Koster MPH, Vasak B, Redman C, Franx A, Georgieva A. Effect of signal acquisition method on the fetal heart rate analysis with phase rectified signal averaging. *Physiol Meas* 2016; **37**: 2245–2259.
27. Graatsma EM, Mulder EJ, Vasak B, Lobmaier SM, Pildner von Steinburg S, Schneider KT, Schmidt G, Visser GH. Average acceleration and deceleration capacity of fetal heart rate in normal pregnancy and in pregnancies complicated by fetal growth restriction. *J Matern Fetal Neonatal Med* 2012; **25**: 2517–2522.
28. Bhide A, Johnson J, Rasanen J, Acharya G. Fetal heart rate variability with hypoxemia in an instrumented sheep model. *Ultrasound Obstet Gynecol* 2019; **54**: 786–790.
29. Weyrich J, Ortiz JU, Müller A, Schmidt G, Brambs CE, Graupner O, Kuschel B, Lobmaier SM. Intrapartum PRSA: a new method of predict fetal acidosis? A case-control study. *Arch Gynecol Obstet* 2020; **301**: 137–142.

SUPPORTING INFORMATION ON THE INTERNET

The following supporting information may be found in the online version of this article:

Table S1 Maternal and fetal characteristics of 285 pregnancies that underwent fetal heart-rate monitoring